Articles

Synthesis and Characterization of Stable Hollow Ti−Silica Microspheres with a Mesoporous Shell

Wenjiang Li and Marc-Olivier Coppens*

DelftChemTech, Delft University of Technology, Julianalaan 136, 2628BL Delft, The Netherlands

Received September 6, 2004. Revised Manuscript Received December 3, 2004

Titanium−silica hollow spheres with a mesoporous shell have been synthesized using an inverse multiple oil−water−oil (O/W/O) emulsion. The oil phase consists of kerosene and sorbitan monooleate (Span 80, $C_{24}H_{44}O_6$); the aqueous phase is a viscous sol solution, prepared from ethanol, Ti−Si species, and HNO_3 solution. The transparent shells are up to several micrometers thick and are interspersed by a random mesopore network with a high specific surface area of 779 m^2/g. This improves the stability and surface permeability of the hollow spheres. FTIR, Raman, and UV−vis spectra suggest that part of the Ti atoms is present as isolated Ti sites in the silica framework, together with amorphous titania oligomers. Applications of this novel material as catalyst or host−guest material are anticipated.

Introduction

Titanium silicate-1 (TS-1), in which titanium is substituted into a silicate framework, shows excellent catalytic properties in a range of mild selective oxidation reactions with aqueous hydrogen peroxide as the oxidant.[1,2] In recent years, a variety of other titanium-containing microporous zeolites,[3] such as TS-2 and Ti-B, as well as mesoporous materials,[4] such as Ti-MCM-41, Ti-HMS, and Ti-MCM-48, have been prepared. Recently, synthesis of functional materials with hollow interiors has attracted much attention because of potential applications in drug storage and release, confined-space catalysis, separation, chromatography, and biomolecular release systems.[5,6] Presently, hollow spheres of various diameters and wall thickness are typically synthesized via layer-by-layer self-assembly of preformed nanoparticles onto spherical particles such as polystyrene beads or silica sol, which are used as templates.[7] However, this is a time-consuming way to obtain the desired layer thickness. An alternative approach involves the direct synthesis of intact inorganic shells around soft templates such as vesicles and emulsion droplets.[8] Schacht et al.[9] first demonstrated that mesoscopically ordered hollow spheres could be prepared by interfacial reactions conducted in oil/water emulsions with varying extents of imposed shear. Huo et al.[10] extended this general emulsion-based approach to prepare spheres with diameters of 0.1−2.0 mm. Tanev and Pinnavaia[11] condensed silica in the interlayer regions of multilamellar vesicles to form roughly spherical particles with stable lamellar mesostructures. Bruinsma et al.[12] and Lu et al.[13] used spray drying to prepare hollow, spherical or collapsed, irregular particles. Despite all these efforts, the various pathways to prepare nominally spherical macrostructured particles have so far resulted in rather irregularly shaped particles, lacking structural stability, or particles with a nonuniform, ill-defined macrostructure.[13] Moreover, the shells are typically too thin for many applications where mechanical strength is an issue.

In this paper, a simple method is described to synthesize thermally stable, mesoporous, hollow spherical shells of

* To whom correspondence should be addressed. Tel: +31-15-2784399. Fax: +31-15-2788713. E-mail: M.O.Coppens@tnw.tudelft.nl.

(1) Taramasso, M.; Perego, G.; Notari, B. (SNAM Progetti S. P. A.) *U. S. P.* 4410501, 1983 [Chem. Abstr. **1981**, *95*, 206272k]. Notari, B. *Catal. Today* **1993**, *18*, 163.
(2) Hölderich, W.; Messe, M.; Nauman, F. *Angew, Chem. Int. Ed. Engl.* **1988**, *27*, 226. Huybrechts, D. R. C.; Vaesen, I.; Li, H. X.; Jacobs, P. A. *Catal. Lett.* **1991**, *8*, 237.
(3) Corma, A.; Navarro, M. T.; Pérez-Pariente, J. *J. Chem. Soc. Chem. Commun.* **1994**, 147. Millini, R.; Perego, G.; Berti, D.; Parker, W. O., Jr.; Carati, A.; Bellussi, G. *Microporous Mesoporous Mater.* **2000**, *387*, 35. Arends, I. W. C. E.; Sheldon, R. A.; Wallan, M. *Angew. Chem., Int. Ed. Engl.* **1997**, *36*, 1144.
(4) Tanev, P. T.; Chibwe, M.; Pinnavaia, T. J. *Nature* **1994**, *368*, 317. Koyano K. A.; Tatsumi, T. *J. Chem. Soc., Chem. Commun.* **1996**, 145. Bagshaw, S. A.; Pouzet, E.; Pinnavaia, T. J. *Science* **1995**, *269*, 1242.
(5) Ringsdorf, H.; Schlarb, B.; Venzmer, J. *Angew. Chem., Int. Ed. Engl.* **1998**, *27*, 113. Sukhorukov, G.; Dähne, L.; Hartmann, J.; Donath, E.; Möhwald, H. *Adv. Mater.* **2000**, *12*, 112. Huang, H.; Remsen, E. E.; Kowalewski, T.; Wooley, K. L. *J. Am. Chem. Soc.* **1999**, *121*, 3805.
(6) Wendland, M. S.; Zimmerman, S. C. *J. Am. Chem. Soc.* **1999**, *121*, 1389. Mdischer, B.; Won, Y.-Y.; Ege, D. S.; Lee, J. C.-M.; Bates, F. S.; Discher, D. E.; Hammer, D. A. *Science* **1999**, *284*, 1143.
(7) Caruso, F.; Shi, X.; Caruso, R. A.; Susha, A. *Adv. Mater.* **2001**, *13*, 740. Bourlinos, B.; Karakassides, M. A.; Petridis, D. *Chem. Commun.* **2001**, 1518.
(8) Huang, J.; Xie, Y.; Li, B.; Liu, Y.; Qian, Y.; Zhang, S. *Adv. Mater.* **2000**, *12*, 808. Imhot, A.; Ping, D. J. *Nature* **1997**, *389*, 948.
(9) Schacht, S.; Huo, Q.; Voigt-Martin, I. G.; Stucky, G. D.; Schüth, F.; *Science* **1996**, *273*, 768.
(10) Huo, Q.; Feng, J. L.; Schüth, F.; Stucky, G. D. *Chem. Mater.* **1997**, *9*, 14.
(11) Tanev, P. T.; Pinnavaia, T. J. *Science* **1996**, *271*, 1267.
(12) Bruinsma, P. J.; Kim, A. Y.; Liu, J.; Baskaran, S. *Chem. Mater.* **1997**, *9*, 2507.
(13) Lu, Y.; Fan, H.; Stump, A.; Ward, T. L.; Reiker, T.; Brinker, C. J. *Nature* **1999**, *398*, 223.

10.1021/cm048486w CCC: $30.25
Published on Web 04/02/2005

Scheme 1. Schematic Drawing of the Suggested Formation Process of a Hollow Structure

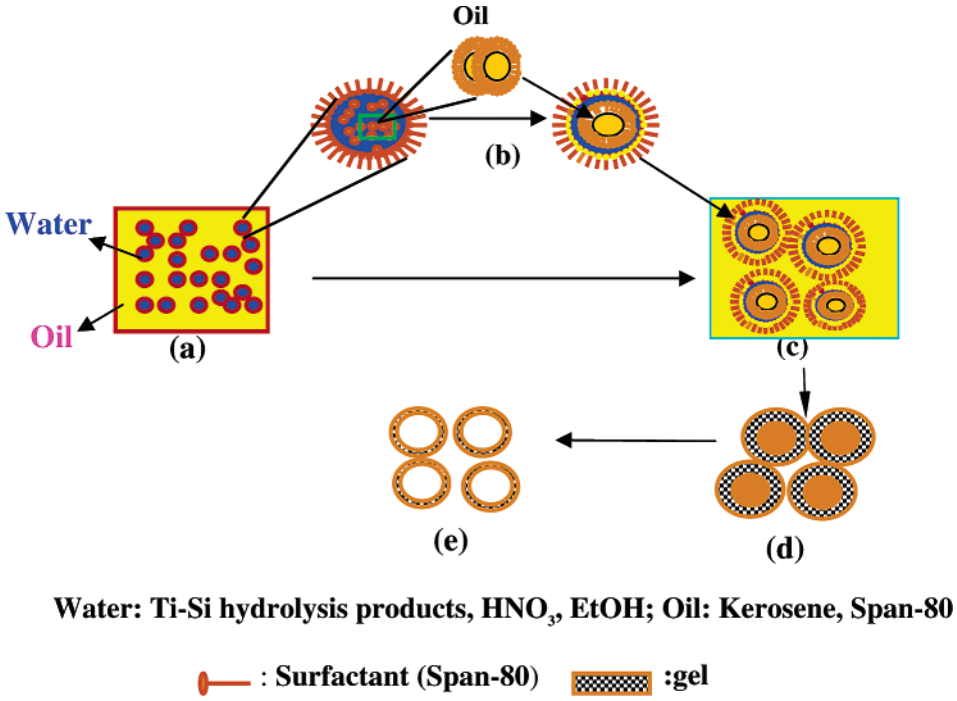

Ti−silica, tens of micrometers in diameter, with part of the titanium as isolated Ti sites, and a very high specific surface area. The environment of Ti is important, since there are indications that, for TS-1, isolated titanium atoms in the framework of the titanium−silica composite are the active sites for selective oxidation.[2] Also useful is the ability to control the thickness of the mesoporous shell, since this impacts permeability and overall catalytic efficiency.

This is accomplished via a synthesis procedure that involves essentially two steps: (1) preparation of a sol solution of Ti−Si precursor by the prehydrolysis of a mixture of tetra-ethyl orthosilicate (TEOS) and $TiO(NO_3)_2$ solutions; and (2) fabrication of a hollow structure of Ti−Si composite via a multiple emulsion method. This method is based upon an inverse multiple (O/W/O) emulsion, which is composed of oil phases O (kerosene, sorbitan monooleate (Span 80, $C_{24}H_{44}O_6$)), and aqueous phases W (the viscous sol solution, containing ethanol, Ti−Si species, and HNO_3 solution). The resulting hollow spheres were characterized by transmission electron microscopy (TEM), scanning electron microscopy (SEM), N_2 sorption, Raman, FTIR, and UV−vis spectroscopy.

Experimental Section

Preparation of a $TiO(NO_3)_2$ and Ti−Si Precursor. First, a white $Ti(OH)_4$ precipitate, formed by mixing 1.0 mL of titanium(IV) *n*-butoxide and 30 mL of water, was filtered and washed with water, then dissolved in 3.0 mL of 4 M HNO_3, thus obtaining a $TiO(NO_3)_2$ solution. Second, 6.6 mL of TEOS, 3.0 mL of $TiO(NO_3)_2$ solution, and 2.0 mL of ethanol were mixed and vigorously stirred for 30 min, forming a homogeneous viscous sol solution of the Ti−Si precursor (containing 9.5 mol % Ti).

Fabrication of Hollow Spheres and Proposed Mechanism. After the above Ti−Si precursor solution was poured into a 200-mL round-bottom glass flask containing 26.1 g of kerosene and 7.9 g of nonionic surfactant Span-80 (sorbitan monooleate) purchased from Aldrich, two separate phases were clearly observed: an oily phase (O) containing the surfactant, on top, and an aqueous solution (W), below. As soon as the two-phase solution was agitated by a homogenizer at a rate of 1000 rpm at 80 °C, a white opaque emulsion appeared due to the formation of water droplets in the oil phase (W/O) (Scheme 1a). In fact, the homogenizer caused each aqueous droplet in the oil phase to also contain many smaller oil droplets (Scheme 1b). Binks et al.[14] reported that the inner drops in such a hierarchical emulsion could totally coalesce to form an oil droplet inside each aqueous droplet, such as to yield a stable multiple emulsion with an oil−water−oil structure (O/W/O). The aqueous phase was therefore confined between the two oil phases. Because of the prehydrolysis of TEOS and Ti species in an acid environment, the aqueous viscous sol (Ti−Si precursor) contained a lot of inorganic nuclei (Si−Ti), which condensed into a solid gel, and formed shells between the outside and inside oil phase (Scheme 1c). After 2 h of emulsification, this resulted in a well-defined "gel shell−oil core" structure. These spherical particles precipitated at the bottom of the glass flask (Scheme 1d). Meanwhile, under acidic conditions, hydrogen bonds between the inorganic nuclei and the nonionic surfactants resulted in the formation of an inorganic−organic mesophase complex at the interfaces of the double emulsion because of the assembly and aggregation of the inorganic Ti−Si nuclei and the surfactant through a neutral S°I° assembly pathway. The products were filtrated, washed with acetone and water, and dried for 3 h at 80 °C. The dispersed hollow spheres were obtained after the organic oil and surfactant were removed by calcination at 700 °C for 6 h (Scheme 1e). Diameters ranging from a few to several tens of micrometers were obtained by changing the synthesis conditions.

Characterization. Thermogravimetric analysis (TGA) was studied on a Perkin-Elmer TGA7, under flowing air at 303−1273 K with a heating rate of 10 K/min. Nitrogen adsorption/desorption isotherms were measured on a Micromeritics ASAP2000 sorption analyzer, utilizing the Barrett−Joyner−Halenda (BJH) method to evaluate the pore volume, surface area, and pore size distributions

(14) Binks, B. P.; Dyab, A. K. F.; Fletcher, P. D. I. *Chem. Commun*. **2003**, 2540.

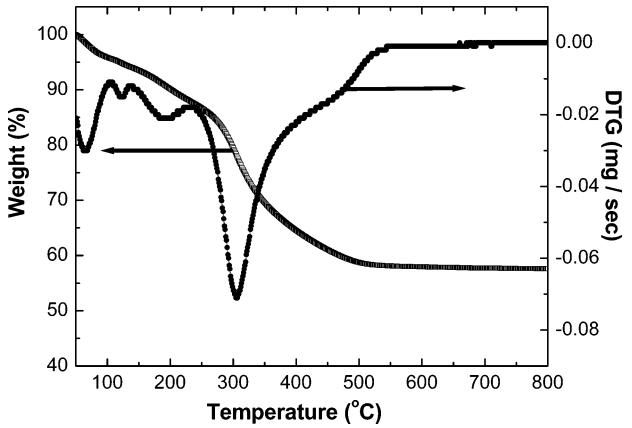

Figure 1. TGA and differential curve of the synthesized hollow spheres.

from the desorption portion of the isotherm. High-resolution transmission electron micrographs were recorded using a Philips CM30T electron microscope with a LaB_6 filament as the electron source, operated at 300 kV. Samples were mounted on a microgrid carbon polymer, supported on a copper grid by placing a few droplets of a suspension of the ground sample in ethanol on the grid, followed by drying at ambient conditions. SEM images were recorded using a Philips XL20. Diffuse reflectance UV/vis/NIR spectra were recorded using a Perkin-Elmer Lambda 19 spectrometer. FTIR spectra on pellets of the samples mixed with KBr were recorded in air with a Bruker IFS88 spectrometer. Raman spectra were obtained using a micro Raman spectrograph, the JY Horiba lab Ram HR 800, excited by a Coherent I-308 argon ion laser emitting 200 mW of power at 488 nm.

Results and Discussion

TGA of the air-dried samples shows a weight loss of about 42% (Figure 1). This mass loss is mainly divided into three temperature regions: below 150 °C, 150−550 °C, and above 550 °C. Mass loss of the samples during heating from 50 to 150 °C corresponds to the loss of ethanol, loosely bound water, and kerosene. Between 150 and 550 °C there are three regions of mass loss associated with three exothermic DTG peaks, which correspond to different stages in the oxidation of Span-80 species, which were formerly dissolved in occluded oil. The peak observed at approximately 190 °C can be ascribed to the decomposition of the organic template, while the peak at 450 °C can be attributed to the combustion of organic residuals, respectively. The gradual loss in mass at higher temperatures could be attributed to the dehydration and condensation of silanols. Thus, anhydrous $Ti-SiO_2$ with a residual mass of 58% was obtained after heating at 700 °C for 6 h. These results suggest that some amount of surfactant Span-80 and kerosene was indeed occluded inside the solid inorganic hollow structures. This is consistent with the proposed mechanism.

Figure 2 shows optical microscopy images of the samples after calcination at 700 °C for 6 h. Dispersed transparent microspheres with a wide size distribution appear on the reflection and transmission images (parts a and b of Figure 2), which show strong contrast between the dark edges and the pale centers of the spherical particles. The magnified reflection image (Figure 2c) reveals that the contrast between the dark edge and the pale center is due to the reflection of light from the outside surface of the spherical particles. On

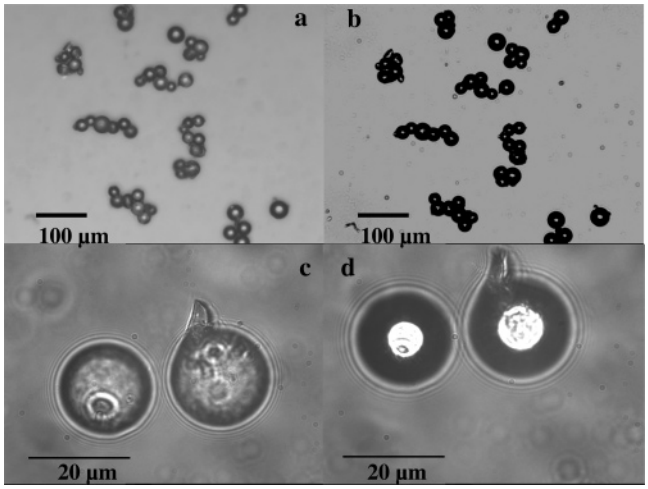

Figure 2. Optical images of the sample in (a) reflection and (b) transmission. (c and d) Corresponding magnified images.

the other hand, contrast in the corresponding transmission image is stronger, because the light pierces through the empty center of the hollow structure. This provides evidence for hollow spheres with a thick shell. It is worth noting that the spheres remain intact and preserve their three-dimensional spherical nature even after calcination at high temperatures. The excellent dispersion of the spheres can be explained by the condensation of inorganic species at the interfaces of the emulsion in a completely isolated environment between the outside and inside oil phase, thus avoiding the agglomeration among different spheres.

SEM studies clearly show a high yield of micrometer-sized spherical structures with a smooth surface texture (Figure 3a). The shells are smooth and intact because, during synthesis, kerosene and decomposition products left the hollow interior via the mesopores in the thick shells. The hollow shell structure was observed as the sample was mechanically fractured with a spatula, showing cavities with a smooth interior, which indicates that the condensation of the inorganic species occurred specifically at the interface of the emulsion droplets (parts b and c of Figure 3). The SEM images of the broken microspheres show that the shell thickness is on the order of a micrometer or more, but may vary with particle size (parts b and c of Figure 3). When hollow spheres of the same size are compared, we found the thickness of the shells to increase with the quantity of TEOS added. Figure 3d shows an image of hollow spheres with a thicker shell as the amount of TEOS was increased from 30 mmol (6.6 mL solution) to 40 mmol (8.8 mL solution), indicating that the shell thickness could be controlled by varying the TEOS concentration. This thicker shell provides the hollow microspheres with a higher thermal and hydrothermal stability, on top of an increased mechanical stability, compared to previously reported hollow spheres.[6,7] Hollow transparent spheres with a thicker shell can be very useful, not only in technical applications but also in the study of physical phenomena, such as optical resonance in a cavity.

The porosity of the shell was investigated by measuring nitrogen adsorption and desorption isotherms at 77 K (Figure 4). The specific surface area according to the Brunauer−Emmett−Teller method is 779 m^2/g, the pore volume is 0.84

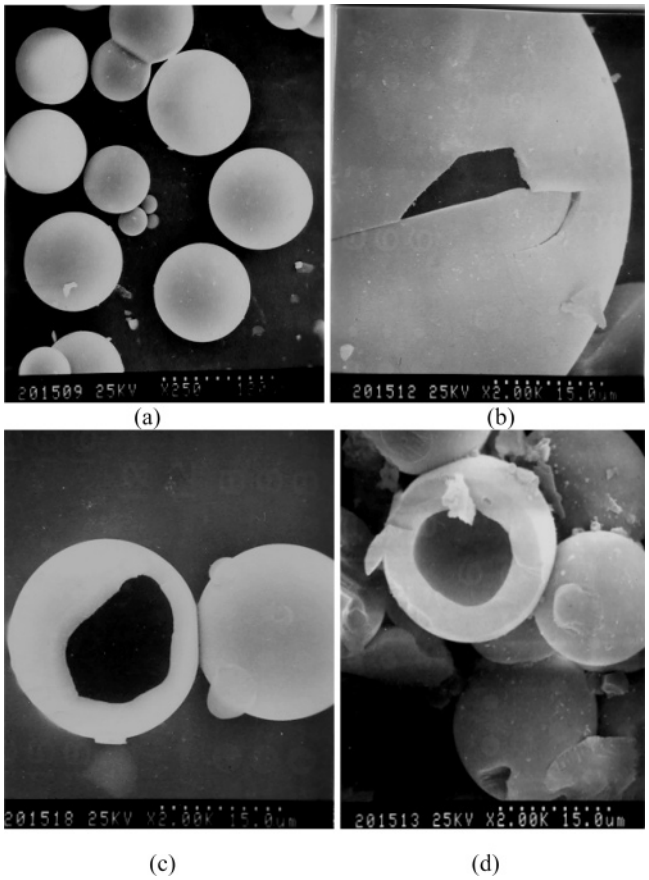

Figure 3. (a) SEM images of the hollow microspheres after calcination at 700 °C (a), (b and c) crushed hollow silica spherical particles, and (d) crushed hollow microsphere prepared using an increased concentration of TEOS.

cm^3/g (for pores between 5 and 10 nm in diameter), and the average pore diameter is 4.1 nm according to the BJH method applied to the desorption branch. The small peak around 3.7 nm is artificial and is a result of the tensile strength effect rather than a bimodal pore size distribution.[15] The mesopores provide pathways by which oil and surfactant can be removed from the interior of the hollow spheres during calcination, without bursting the shells. This is in agreement with previously reported pure silica hollow spheres.[16] The TEM image confirms the mesoporous structure of the shells (Figure 5). It shows a disordered structure with random pore orientation, similar to that of certain other silica materials templated by neutral surfactants.[17] Consistent with the TEM image, the X-ray diffractogram (not shown) is featureless and typical for mesoporous materials with a poorly ordered mesostructure. In our experiments the surfactants Span-80 and the inorganic Ti−Si species could be assembled at the emulsion interface into mesostructured organic−inorganic complexes by hydrogen bonding, according to a neutral (S°I°) assembly pathway. Hollow spheres fabricated by using this emulsion as template usually consist of a porous rather than a dense shell.

Both amorphous and crystalline binary titanium−silica materials have useful physical and chemical properties. For example, dense amorphous titanium−silica glass has a significantly higher refractive index than fused quartz, which depends on the titanium concentration, and has an anomalously low coefficient of thermal expansion.[18,19] These properties have led to commercial exploitation as thin film and bulk optical materials. Furthermore, porous titanium silicalite (TS-1) zeolites and xerogels are active and selective catalysts in a number of low-temperature oxidation reactions with aqueous H_2O_2 as the oxidant.[20] For their relevance in industrial applications, they have been some of the most studied heterogeneous catalysts in recent years.

In our work, Ti is introduced into the silica substrate through the cohydrolysis of a mixed solution of TEOS and $TiO(NO_3)_2$; Ti species react with the silica substrate to form a Ti−O−Si structure after calcination. Structural information is very important for applications and can be investigated spectroscopically.[21] The UV−vis spectrum of Ti−silica hollow spheres calcined at 700 °C shows a broad absorption band near 215 nm together with a weak shoulder band at 275 nm (Figure 6). The bands at lower wavelengths can be assigned to an electronic charge-transfer transition associated with an isolated Ti(IV) framework site in tetrahedral coordination.[22] Compared with the spectrum of TS-1, which generally gives a narrow absorption band at 210 nm, the red shift and the increased width of the band at 215 nm for Ti−silica hollow spheres may be an indication of Ti in a distorted tetrahedral environment, which is similar to the Ti-MCM-41 reported by Yu et al.[23] This distorted environment is a direct consequence of the amorphous character of the pore walls, yielding a wide range of Ti−O−Si bond angles.[24] The broad band around 275 nm shows partially polymerized Ti species containing Ti−O−Ti bonds in the silicon-rich amorphous phase.[25] The weak absorption band characteristic of octahedral extraframework titanium at 330−340 nm further suggests the presence of Ti−O−Ti units. Amorphous TiO_2/SiO_2 gels with various Ti contents exhibit absorption bands in the intermediate range of 250−350 nm.[26] Overall, the spectrum points toward the presence of amorphous titania oligomers, apart from isolated Ti sites. The XRD pattern of the Ti−silica sample calcined at 700 °C for 6 h clearly shows an amorphous phase (insert of Figure 6) and indicates the absence of bulk anatase crystals. The above results suggest that, while part of the Ti^{4+} isomorphically

(15) Groen, J. C.; Peffer, L. A. A.; Perez-Ramirez, J. *Microporous Mesoporous Mater.* **2003**, *60*, 1.
(16) Li, W. J.; Sha, X. X.; Dong, W. J.; Wang, Z. C. *Chem. Commun.* **2002**, 2434.
(17) Sing, K. S. W.; Everett, D. H.; Haul, R. A. W.; Moscou, L.; Pierotti, R. A.; Rouquerol, J.; Siemieniewska, T. *Pure Appl. Chem.* **1985**, *57*, 603. Tanev, P.; Pinnavaia, T. *Science* **1995**, *269*, 1242.
(18) McCulloch, S.; Stewart, G.; Guppy, R. M.; Norris, J. O. W. *Int. J. Optoelectron.* **1994**, *9*, 235.
(19) Evans, D. L. *J. Am. Ceram. Soc.* **1970**, *53*, 418.
(20) Davis, R. J.; Liu, Z. F. *Chem. Mater.* **1997**, *9*, 2311.
(21) Taramasso, M.; Perego, G.; Notari, B. U.S. Patent 4,410,501, 1983. Taramasso, M.; Manara, G.; Fattore, V.; Notari, B. U.S. Patent 4,-666,692, 1987.
(22) Petrini, G.; Cesana, A.; De Alberti, G.; Genoni, F.; Leofanti, G.; Paclovan, M.; Paparatto, G.; Rofia, P. *Stud. Surf. Sci. Catal.* **1991**, *68*, 761.
(23) Yu, J. Q.; Feng, Z. C.; Xu, L.; Li, M. J.; Xin, Q.; Liu, Z. M.; Li, C.; *Chem. Mater.* **2001**, *13*, 994.
(24) Zhang, W.; Froba, M.; Wang, J.; Tanev, P. T.; Wong, J.; Pinnavaia, T. J.; *J. Am. Chem. Soc.* **1996**, *118*, 9164.
(25) Blasco, T.; Corma, A.; Navarro, M. T.; Perez-Pariente, J. *J. Catal.* **1995**, *156*, 65. Anpo, M.; Nakaya, H.; Kodama, S.; Kubokawa, Y. *J. Phys. Chem.* **1986**, *90*, 1633.
(26) Notari, B. *Stud. Surf. Sci. Catal.* **1988**, *37*, 413.

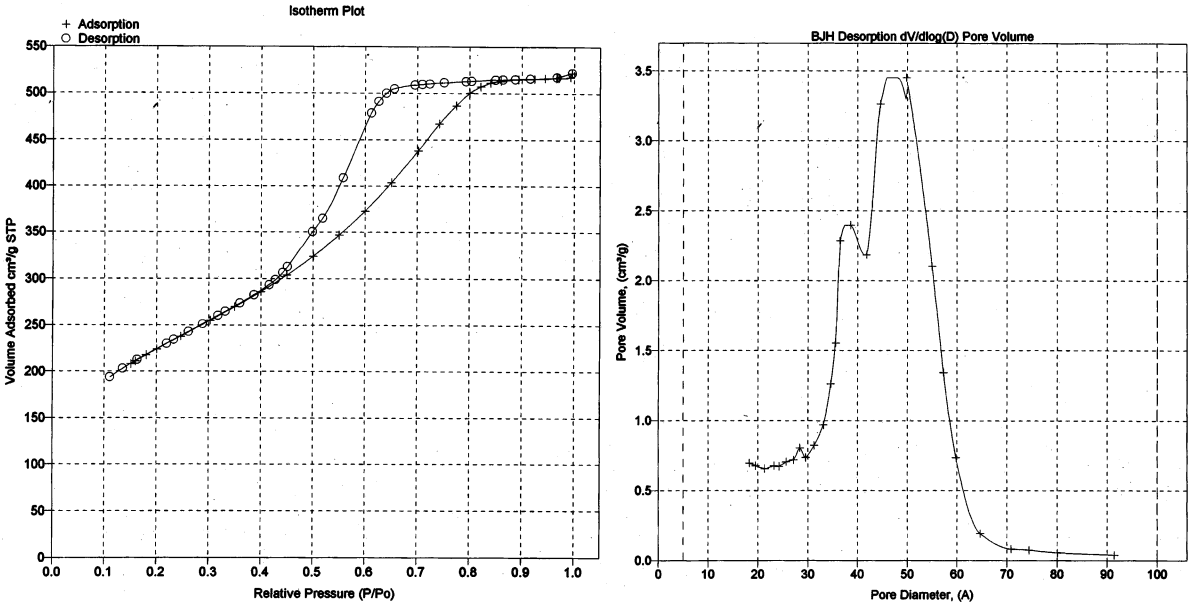

Figure 4. (a) Adsorption−desorption isotherm of nitrogen at 77 K on the calcined samples. (b) Pore-size distribution calculated from the desorption branch of the isotherm, using the BJH method.

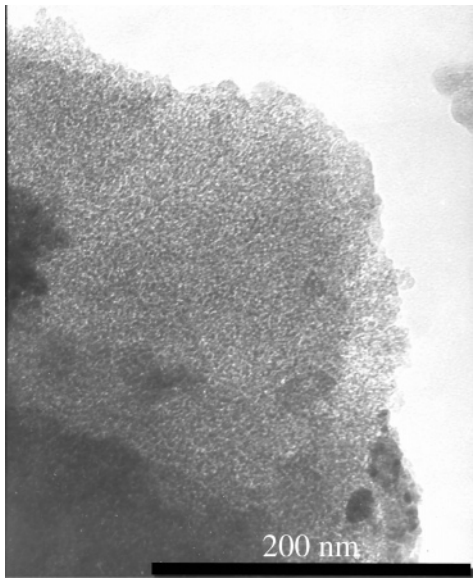

Figure 5. TEM image of a crushed, calcined spherical particle.

substituted Si^{4+} in the silica framework of Ti−silica hollow spheres to form a Ti−O−Si structure, other Ti atoms are present in Ti−rich microdomains with Ti−O−Ti linkages.[27]

Additional support for this conjecture comes from vibrational spectroscopy. Figure 7 shows the FTIR spectra of pure silica and titania−silica hollow spheres. Interestingly, only the Ti-containing sample shows a peak at about 950 nm, which is due to Ti−O−Si species,[28] indicating that some Ti condensation with the siliceous species occurred at this stage. This is in good agreement with the diffuse reflectance UV result and confirms that some Ti is chemically bonded to silica.[29]

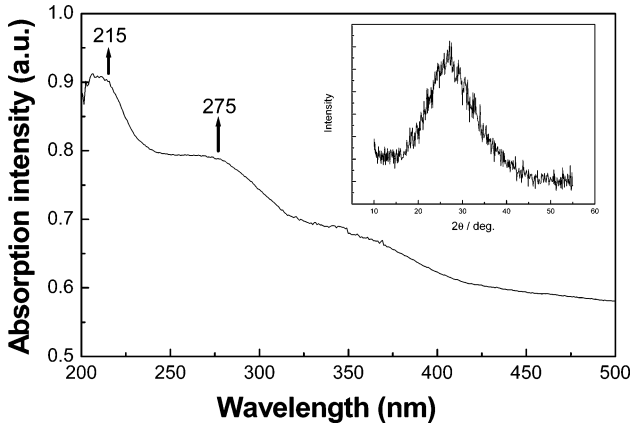

Figure 6. UV−vis spectrum of Ti−silica hollow spheres. Insert shows corresponding XRD pattern.

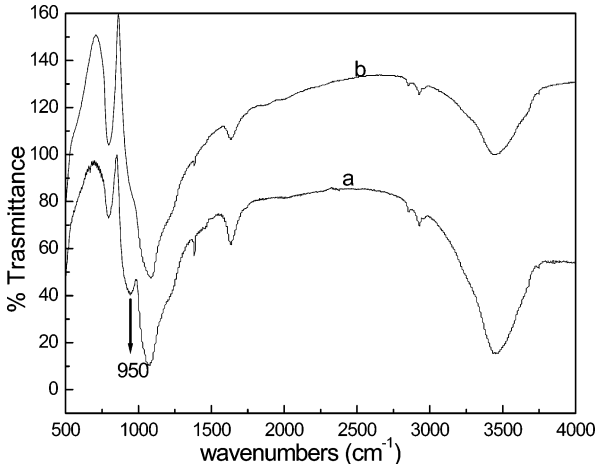

Figure 7. FTIR spectra of (a) Ti−silica composite hollow spheres calcined at 700 °C and (b) a pure silica sample calcined at 700 °C.

Raman spectra of the Ti−silica hollow spheres, calcined at 700 °C, and of anatase are presented in Figure 8. Anatase is known to have strong Raman scattering properties[30] with intense Raman bands at about 150, 395, 515, and 640 cm^{-1} as shown in curve b of Figure 8. In contrast to anatase, the

(27) Dutoit, M. D. C.; Schneider, M.; Baiker, A. *J. Catal.* **1995**, *153*, 165. Klein, S.; Thorimbert, S.; Maier, W. F. *J. Catal.* **1996**, *163*, 476.
(28) Marchese, L.; Gianotti, E.; Dellarocca, V.; Maschmeyer, T.; Rey, F.; Coluccia, S.; Thomas, J. M. *Phys. Chem. Chem. Phys.* **1999**, *1*, 585.
(29) Soult, A. S.; Carter, D. F.; Schreiber, H. D.; van de Burgt, L. J.; Stiegman, A. E. *J. Phys. Chem. B* **2002**, *106*, 9266.

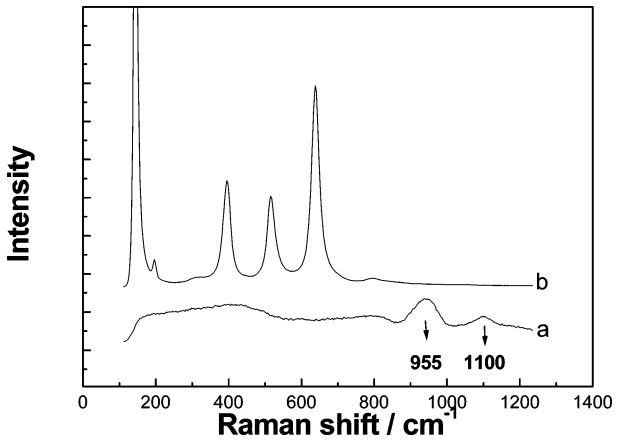

Figure 8. Raman spectra of (a) Ti−silica composite hollow spheres calcined at 700 °C and (b) pure anatase TiO_2.

synthesized sample (curve a in Figure 8) shows very weak Raman spectra. The calcined sample at 700 °C shows no trace of the 150 cm^{-1} bands, which is a sensitive indicator of the presence of anatase, consistent with the XRD pattern. This indicates the absence of bulk titania.[31] On the other hand, there clearly are titanium-dependent bands at 955 and 1100 cm^{-1}, corresponding to a symmetric stretch and an antisymmetric stretch, respectively.[32]

From the UV−vis spectra along with the FTIR and Raman spectra, it is deduced that most Ti in the shell is not present in a bulk anatase phase and that both amorphous titania oligomers and isolated Ti sites are present in the silica. It was also found that a higher Ti concentration in the Ti precursor solution resulted in the formation of a bulk titania phase in the shell, similar to findings reported by Kosuge and Singh.[33]

Conclusion

A new method was introduced to synthesize transparent, thermally stable, hollow titanium−silica microspheres by using an inverse O/W/O emulsion technique. By a change in the concentration of the silica source, the shell thickness could be controlled. A thick shell with a large specific area interspersed by a random mesopore network improves the stability and surface permeability of the hollow spheres. TEM and N_2 sorption show that typical samples have a disordered egg-shell-like mesoporous structure. Specific surface area, pore volume, and average pore diameter of the discussed sample are 779 $m^2\ g^{-1}$, 0.84 cm^3/g, and 4.1 nm, respectively. FTIR, Raman, and UV−vis spectra indicate that Ti atoms are successfully incorporated as isolated Ti sites into the silicate framework. The titanium silicate microspheres maintain their hollow shell architecture even when heated to 700 °C for 6 h.

This new inverse multiple-emulsion-based synthesis method leading to stable titanium silicate hollow spheres is of interest to catalysis but also to other potential applications such as controlled release capsules for drugs, dyes, cosmetics and inks, artificial cells, and fillers. Increased monodispersity of the shells should make them interesting candidates for a new class of building blocks to fabricate colloidal crystals that are expected to exhibit improved photonic band gap properties.[34] As a result, the next challenge is to make even more uniform hollow spheres using this inverse multiple emulsion method.

Acknowledgment. We thank Dr. P. J. Kooyman for the TEM measurements, and Mr. J. C. Groen for helpful discussion about the N_2 sorption measurement interpretation. This work was made possible thanks to funding from TU Delft and the Dutch National Science Foundation, NWO, via a PIONIER award.

CM048486W

(30) Davis, R. J.; Liu, Z. *Chem. Mater.* **1997**, *9*, 2311. Liu, Z.; Davis, R. J. *J. Phys. Chem.* **1994**, *98*, 1253.

(31) Gao, X.; Bare, S. R.; Fierro, J. L. G.; Banares, M. A.; Wachs, I. E. *J. Phys. Chem. B* **1998**, *102*, 5653. Miller, J. M.; Lakshmi, L. J. *J. Phys. Chem. B* **1998**, *102*, 6465.

(32) Ricchiardi, G.; Damin, A.; Bordiga, S.; Lamberti, C.; Spano, G.; Rivetti, F.; Zecchina, A. *J. Am. Chem. Soc.* **2001**, *123*, 11409. Knight, D. S.; Pantano, C. G.; White, W. B. *Mater. Lett.* **1989**, *8*, 156.

(33) Kosuge, K.; Singh, P. S. *J. Phys. Chem. B* **1999**, *103*, 3563.

(34) Xia, Y.; Gates, B.; Yin, Y.; Lu, Y. *Adv. Mater.* **2000**, *12*, 693.